Molecular dynamics simulation of structural change at metal/semiconductor interface induced by nanoindenter*

Bing-Bing Zhao(赵兵兵)[1,2], Ying Wang(王影)[1,2], Chang Liu(刘畅)[1,2], and Xiao-Chun Wang(王晓春)[1,2,†]

[1] *Institute of Atomic and Molecular Physics, Jilin University, Changchun* 130012, *China*

[2] *Jilin Provincial Key Laboratory of Applied Atomic and Molecular Spectroscopy, Jilin University, Changchun* 130012, *China*

(Received 16 January 2016; revised manuscript received 27 May 2016; published online 28 September 2016)

The structures of the Si/Cu heterogenous interface impacted by a nanoindenter with different incident angles and depths are investigated in detail using molecular dynamics simulation. The simulation results suggest that for certain incident angles, the nanoindenter with increasing depth can firstly increase the stress of each atom at the interface and it then introduces more serious structural deformation of the Si/Cu heterogenous interface. A nanoindenter with increasing incident angle (absolute value) can increase the length of the Si or Cu extended atom layer. It is worth mentioning that when the incident angle of the nanoindenter is between −45° and 45°, these Si or Cu atoms near the nanoindenter reach a stable state, which has a lower stress and a shorter length of the Si or Cu extended atom layer than those of the other incident angles. This may give a direction to the planarizing process of very large scale integration circuits manufacture.

Keywords: molecular dynamics, metal/semiconductor interface, reconstruction, nanoindenter

PACS: 46.55.+d, 62.25.–g, 68.35.–p **DOI:** 10.1088/1674-1056/25/11/114601

1. Introduction

With the rapid development of computer, telecommunication, and network technologies, the demand for integrated circuits (ICs) has increased. ICs have continued to develop high speed, high integration, high density, and high performance. This leads to smaller size ICs and a narrower distance between the neighboring wiring. Currently, the very large scale integration circuit (VLSI) has reached the 14 nm node. Meanwhile, the number of wiring layers has increased and the width of the metal line has narrowed. Copper has high thermal and electrical conductivity and a high melting temperature when compared to aluminum. Therefore, Cu has become the current VLSI multilayer wiring metal. The Si/Cu heterogenous interface has gained extensive attention for micro-electronic devices. The structural and morphological properties of the Cu template layers grown epitaxially on Si substrates have been studied by Vaz *et al.*[1] in order to provide a better understanding of the characteristics related to the magnetism of ultrathin films. Molecular dynamics (MD) simulation has been used to systematically study the critical conditions of epitaxy, interface mixing, and sputtering for Cu cluster depositing on Si substrate under different incident energies, substrate temperatures, and atom number per cluster.[2] In these studies,[1] the Si/Cu interface is parallel to the surface. As far as we know, few researchers have studied a system where the Si/Cu interface is vertical to the surface.

In addition, chemical mechanical polishing (CMP)[3,4] has drawn great attention as a technique used in semiconductor fabrication for planarizing a semiconductor wafer. MD simulations of the nanoscale polishing of a single-crystal copper surface have been performed to study chip formation, material defects, and frictional forces by Ye *et al.*[5,6] Han *et al.* carried out a nano-scale polishing experiment of silicon wafer using the MD simulation method.[7,8] It was shown that the ductile material removal mode induced by physical phase transformation was the most important factor in achieving high levels of global and local planarities. Lina *et al.*[9,10] proved that both abrasive sliding and rolling play important roles in material removal in the abrasive CMP of the silicon substrate by using the MD simulation method. These studies of CMP of semiconductor are focused on a single copper or silicon surface. Few studies have focused on the CMP of Si/Cu heterogenous interface using the MD simulation method. The manufacture of VLSI with a multilayer structure needs the process of planarizing the surface of the Si wafer embedded with copper wires, which are neighboring by about 10 nm distance. The CMP process will affect the structure of the Si/Cu heterogenous interface which is vertical to the wafer surface, and then affects the performance of the VLSI. However, there are very few investigations of the Si/Cu heterogenous interface which is vertical to the wafer surface using the MD simulation method.

In this paper, we use the MD simulation to study the structural change at the Si/Cu heterogenous interface induced by a nanoindenter. The Si/Cu heterogenous interface is vertical to the surface. This calculation model is set up in order to sim-

*Project supported by the Tribology Science Fund of State Key Laboratory of Tribology, China (Grant No. SKLTKF12A01), the National Natural Science Foundation of China (Grant No. 11474123), the Natural Science Foundation of Jilin Province of China (Grant No. 20130101011JC), and the Fundamental Research Funds for Central Universities at Jilin University, China.

†Corresponding author. E-mail: wangxiaochun@jlu.edu.cn

© 2016 Chinese Physical Society and IOP Publishing Ltd

ulate the mechanical wear of the wafer surface with the Si/Cu heterogenous interface. The mechanical wear is introduced by abrasive particles in the CMP process. We systematically discuss the structural change at the Si/Cu interface induced by nanoindenter with different depths varying from 0 Å to 20 Å and different incident angles varying from -80° to 80°.

2. Computational method and details

The MD simulations are performed using the large-scale atomic/molecular massively parallel simulator (LAMMPS) package.[11] Initially, the simulation model of the Si/Cu heterogenous interface contains about 17200 atoms with a dimension of 217.2 Å×108.06 Å×10.86 Å along x, y, and z directions, respectively. There are 6400 Si atoms and 10800 Cu atoms. At the heterogenous interface, the Si and Cu are in contact via their (100) faces, which are initially separated by 3.16 Å. The Si atoms are initially arranged in a diamond cubic structure with a lattice constant of 5.43 Å, and the Cu atoms are initially arranged in a face center cubic structure with a lattice constant of 3.61 Å. The many-body Tersoff potential[12–14] and the embedded atom method (EAM) potential[15–21] are adopted for the Si–Si and Cu–Cu interactions, respectively. The interfacial interactions between the Si and Cu atoms are described by the Morse two-body potential function[2,22]

$$U = D[\mathrm{e}^{-2\alpha(r-r_0)} - 2\mathrm{e}^{-\alpha(r-r_0)}], \tag{1}$$

where $D = 0.9$ eV, $\alpha = 1.1$ Å^{-1}, and $r_0 = 3.15$ Å. The initial crystal structure of the heterogenous interface of Si/Cu is shown in Fig. 1(a).

In order to attain the minimum interfacial energy and obtain the stable structure of the heterogeneous interface, the following simple scheme is performed. Firstly, the periodic boundary condition (PBC) is used in the x, y, and z directions, and the relaxed system is obtained under zero pressure and constant temperature (300 K) via the isothermal-isobaric ensemble (NPT)[23–26] for 100 ps with a time step of 1 fs, as shown in Fig. 1(b). Then, in order to eliminate the effect of the neighbor heterogeneous interface, the atoms within 8 Å of the edges at the left and right sides along the x axis are completely removed. In the following, the free boundary conditions are imposed in the x and y directions and the periodic boundary condition is applied in the z direction. The Nosé–Hoover thermostat[27,28] is applied, and the structure is equilibrated after 10 ps, which is shown in Fig. 1(c). Then, a few atomic layers within 10 Å of the boundary are fixed at the left, the right, and the bottom edges of the heterogenous interface system.

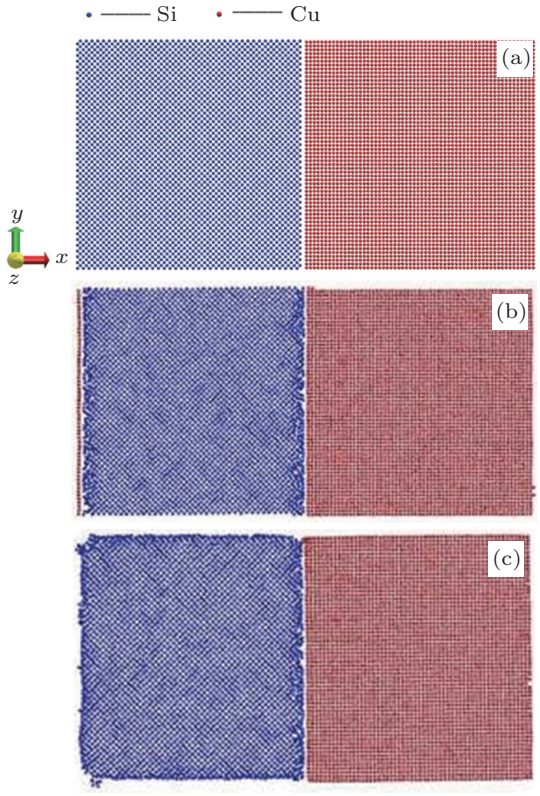


Fig. 1. (color online) Orthographic views of the structures: (a) the initial crystal structure, (b) the structure relaxed via the isothermal-isobaric ensemble (NPT), (c) the structure at equilibrium. The blue and brown spheres represent Si and Cu atoms respectively.

Figure 2 illustrates the nanoindenter incident angle with signs of plus and minus. A cylindrical nanoindenter is modeled exerting a repulsive force

$$F = -K(r-R)^2 \tag{2}$$

on each atom, where K is the specified force constant, r is the distance from the atom to the center axis of the cylinder, and $R = 20$ Å is the radius of the nanoindenter. The cylinder extends infinitely along its axis, which is parallel to the z axis. Indenting is applied with looping. Energy minimization

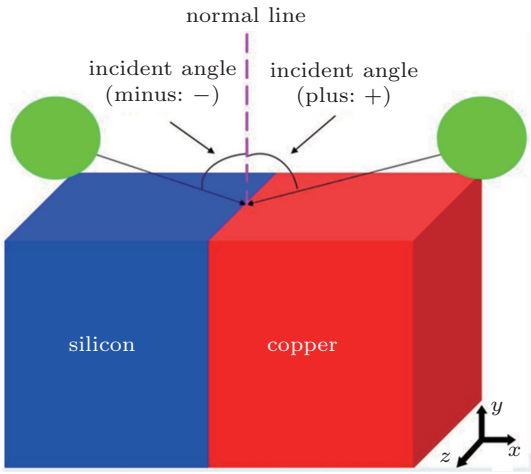


Fig. 2. (color online) The nanoindenters (green spheres) with different incident angles on the Si/Cu heterogenous interface.

is applied. We use the repulsive force to describe the action of the nanoindenter on the surface atoms because it can effectively exclude the effects due to different materials and different surface roughness of the nanoindenter. It can then contribute to reveal the intrinsical interaction mechanism between the nanoindenter and the Si/Cu heterogenous interface.

3. Results and discussion

3.1. The extended atom layer of Si or Cu under the nanoindenter

The aim of the present study is to reveal the formation mechanism of the structural change at the surface of the heterogenous interface under the nanoindenter with different incident angles. The incident angles between the normal line and the incident direction of the loading nanoindenter are $\pm 80°$, $\pm 70°$, $\pm 60°$, $\pm 45°$, $\pm 30°$, and $0°$ for this study, and the nanoindentation depth is chosen as 20 Å. The relaxed structures with different incident angles are shown in Fig. 3. The reconstruction phenomenon due to dislocation mainly occurs at the area with obvious accumulation of Si or Cu atoms, where it is pressed by the nanoindenter. For the incident angles less than $0°$, the nanoindentation first breaks the atomic bonds between the surface silicon atoms and the inner ones, and then some of the surface atoms move together with nanoindentation. A similar phenomenon was found in Dan Guo's research of the nanoscratching processes on the surface of single crystalline silicon.[9]

We calculate the length of the extended atom layer under the nanoindenter with different incident angles. The length of the extended atom layer is defined as the length of the atom layer that crosses the plane of the heterogenous interface and reaches to the other side of the plane. The bonds of the Si and

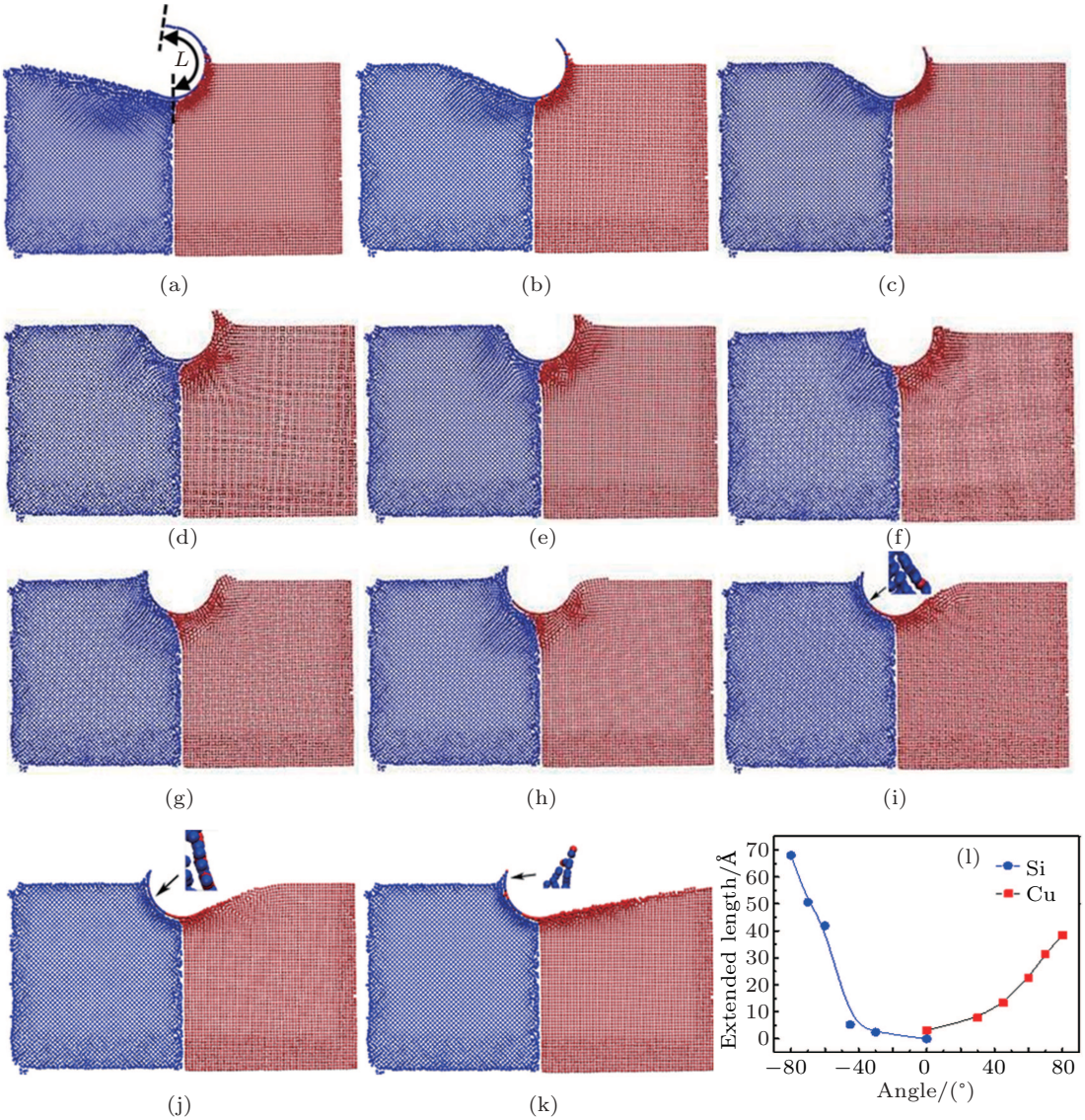


Fig. 3. (color online) MD simulation results showing cross-sectional views of *xy* plane with the same nanoindentation depth (20 Å) and different incident angles: (a) $-80°$, (b) $-70°$, (c) $-60°$, (d) $-45°$, (e) $-30°$, (f) $0°$, (g) $30°$, (h) $45°$, (i) $60°$, (j) $70°$, and (k) $80°$. The extended length L of the extended atom layer is illustrated in panel (a). (l) The lengths of the extended atom layer for different incident angles (blue and red points for the lengths of the Si and Cu extended atom layers, respectively).

Cu atoms near to the nanoindenter are broken under the pressure of the nanoindenter, and the atoms reconstruct in order to reach a new stable state. The lengths of the Si extended atom layer are about 68.06 Å, 50.59 Å, 41.87 Å, 5.23 Å, 2.44 Å, and 0 Å for incident angles of −80°, −70°, −60°, −45°, −30°, and 0°, respectively. The lengths of the Cu extended atom layer are about 3.14 Å, 7.68 Å, 13.26 Å, 22.68 Å, 31.42 Å, and 38.38 Å for incident angles of 0°, 30°, 45°, 60°, 70°, and 80°, respectively. The Si and Cu extended atom layers are almost located around the surface of the nanoindenter (shown in Fig. 3), the configurations of the Si and Cu extended atom layers are related to the radius size of the nanoindenter. The larger radius of the nanoindenter will lead to the longer extended atom layers. In particular, when the incident angle is 80°, the length of the Cu extended atom layer is about 38.38 Å, which is larger than the radius of the nanoindenter. This fact is important for the polishing process of VLSI manufacture. If the radius of the abrasive particles is larger than the distance between the neighboring Cu wires, the Cu extended atom layer may cross the Si surface and reach the neighbor Cu wire surface. This will destroy the electric stability of the wafer. The IC manufacture progress should avoid this phenomenon in order to ensure the high quality of the IC. When Cu is wired on the IC board, the distance of the neighbor copper wires cannot be too short. The radius of each abrasive particle should be smaller than the distance of the neighbor copper wires on the IC board to avoid overlapping the neighboring copper wires. For a certain incident angle, the area of the reconstruction region around the metal/semiconductor interface gradually becomes wider and deeper when the nanoindentation depth increases. For example, for the 0° incident angle, the width of the reconstruction region under the nanoindentation changes to 41.75 Å, 44.97 Å, and 59 Å, and the depth of the region changes to 21.61 Å, 35.97 Å, and 41.02 Å, when the nanoindentation depth is 10 Å, 15 Å, and 20 Å, respectively. Those atoms beyond the reconstruction region keep their sites of bulk structure.

Figure 3(l) clearly shows that the length of the Si or Cu extended atom layer at the surface near the interface will increase with increasing incident angle. The data indicate that the length of the Si extended atom layer (when the incident angle is −80°) is longer than that of Cu (when the incident angle is 80°). When the incident angles are ±70° and ±60°, the situation is similar to that of ±80°. This phenomenon happens because the covalence bonds between Si atoms have stronger directionality than the metallic bonds between Cu atoms. The stress forces will then accumulate around the covalence bonds and lead to the broken covalence bonds. The broken bond Si atoms attach to the moving nanoindenter and form the longer extended atom layer. Figure 3 shows that the length of the Si extended layer decreases rapidly when the incident angle decreases. This happens because the Si surface area affected by the nanoindenter decreases rapidly, and then the number of the broken bond Si atoms is reduced. The Si surface reconstruction gradually becomes the main phenomenon when the incident angle decreases.

3.2. The stress of atoms under the nanoindenter with different incident angles

The distributions of stress of the atoms in the Si/Cu heterogenous interface system are shown in Figs. 4 and 5 for a series of cases with different incident angles (±80°, ±70°, ±60°, ±45°, ±30°, and 0°) and different nanoindentation depths (10 Å, 15 Å, and 20 Å). The reconstruction phenomenon occurs in the red and yellow areas with large stress. As for the situations with 20 Å nanoindentation depth, the reconstruction area in Figs. 4 and 5 is the same as that in Fig. 3 when the incident angle is the same as that in Fig. 3.

The formation mechanism of these reconstruction areas is analyzed in detail as follows. Firstly, when the incident angle is less than −45° or more than 45°, the stress of each atom is increased when the nanoindentation depth is increased. The nanoindenter with increasing depth can lead to the compressing space under the nanoindenter, and then cause the Si or Cu reconstruction. However, when the incident angle is −45°, the nanoindentation with increased depth could lead to that the stress of each atom near the nanoindenter first increases and

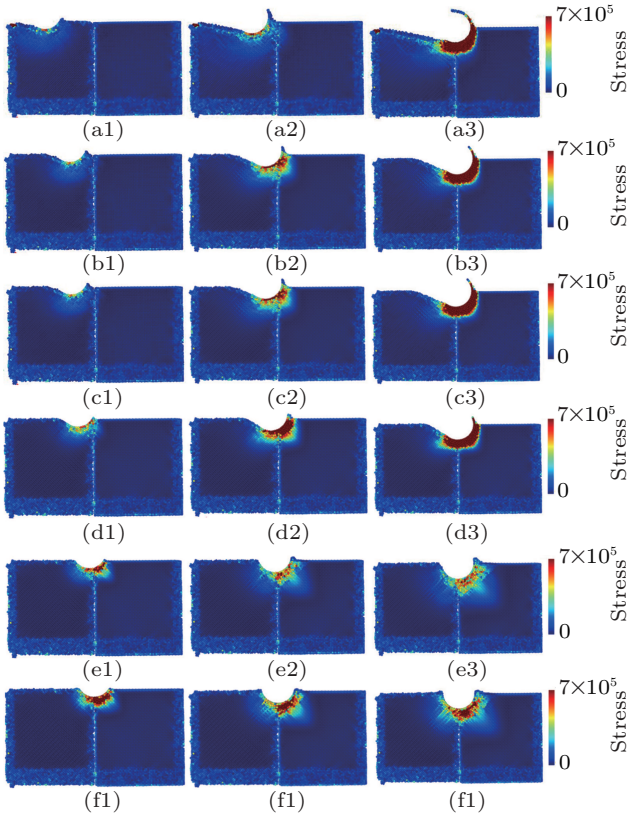


Fig. 4. (color online) The stress distributions of each atom under the nanoindenter with different incident angles ((a) −80°, (b) −70°, (c) −60°, (d) −45°, (e) −30°, and (f) 0°) and different nanoindentation depths ((a1) 10 Å, (a2) 15 Å, (a3) 20 Å).

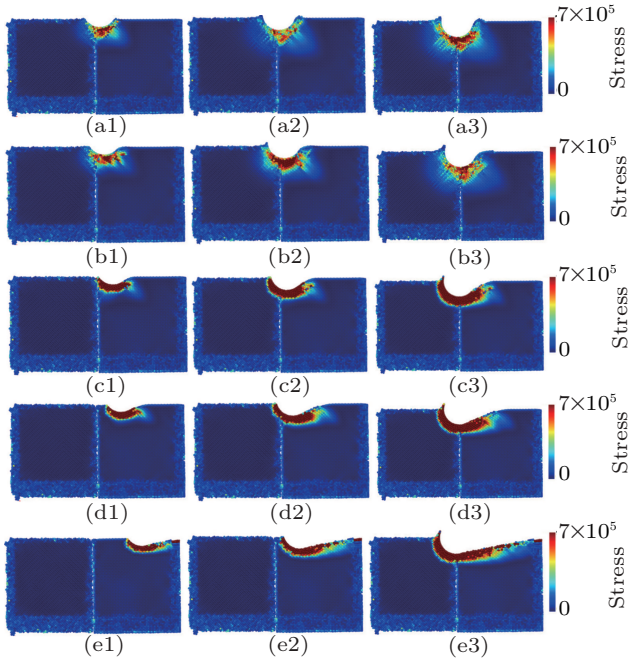


Fig. 5. (color online) The stress distributions of each atom under the nanoindenter with different incident angles ((a) 30°, (b) 45°, (c) 60°, (d) 70°, (e) 80°) and different nanoindentation depths ((a1) 10 Å, (a2) 15 Å, (a3) 20 Å).

then decreases, as shown in Fig. 4(d). A similar phenomenon occurs when the incident angle is 45°. Secondly, for cases with 20 Å nanoindentation depth and the incident angle between −45° and 45°, the stresses on these atoms under the nanoindenter are smaller than those with the incident angle less than −45° or more than 45°. For cases with the incident angle between −45° and 45°, the vertical components of the nanoindenter pressure are larger than those in the case with the incident angle outside the range between −45° and 45°, and the dislocation among these atoms under the nanoindenter can get enough energy to overcome the potential barrier of diffusion. The potential barrier means that the forces from the bulk atoms that prevent the dislocation under the nanoindenter move to the inside of the bulk. The dislocation near the nanoindenter can then diffuse into the deeper region of the material and cause a larger region of dislocation diffusion, as shown in Figs. 4(d3), 4(e3), 4(f3), 5(a3), and 5(b3). The stresses on these atoms are then partly released. These atoms reach a new balance state. Figures 3–5 also show that the dislocation near the nanoindenter diffuses among Si or Cu bulk atoms more easily than among Si and Cu interface atoms. However, when the incident angle is less than −45° or more than 45°, the vertical components of the nanoindenter pressure are smaller than those of the cases with the incident angle between −45° and 45°, and then dislocation among the atoms under the nanoindenter cannot get enough energy to overcome the potential barrier and the dislocation near the nanoindenter is blocked in the small region that is very close to the nanoindenter. The structure of the heterogenous interface system then retains the special state with the stress that cannot be released.

3.3. The radial distribution function under the nanoindenter

The radial distribution function (RDF) is generally used to classify the crystal structure and show the structure change of the crystal system in MD simulations. The RDF is an example of the pair correlation function, which describes how, on average, the atoms in a system are radially packed around each other. The RDF $g(r)$ gives the probability of finding a particle in the distance r from another particle.[29] Figure 6 shows the RDF for the structures of the heterogenous interface system under the nanoindenter with 20 Å nanoindentation depth and different incident angles.

As for the RDF of Si in the heterogenous interface system under the nanoindenter, when the incident angle is from −80° to 45°, there is a slightly raised peak (located at 3.18 Å) between the first peak (located at 2.34 Å) and the second peak (located at 3.82 Å), which is marked in Figs. 6(a)–6(h) respectively. This slightly raised peak is contributed by the reconstruction Si atoms. The stress of the Si surface atoms under the nanoindenter partly transfers to the deep area of the Si material through the strong covalent bond between the Si atoms, which leads to the reconstruction of Si. The height of this peak is 2.15 when the incident angle is −80°, which is higher than 0.92 when the incident angle is −60°. When the incident angle is −80°, the nanoindenter passes through a larger surface area of Si than that when the incident angle is −60°. The number of reconstruction Si atoms due to the nanoindenter for −80° incident angle is larger than that for −60°. However, the raised small peak for the −45° incident angle is 1.47, which is also higher than that for the −60° incident angle. The vertical component of the Si atom stress introduced by the nanoindenter with the −45° incident angle is larger than that with the −60° incident angle. The dislocation of these atoms for −45° can then get enough energy to overcome the potential barrier of diffusion, and diffuses into the material to enlarge the reconstructed area, which is also clearly shown at Fig. 4(d3). As a result, the number of reconstructed Si atoms for the case with the −45° incident angle is larger than that of the case with the −60° incident angle.

As for the RDF of Cu, the first highest peak locates at 2.56 Å, which corresponds to the nearest neighboring Cu atoms in the ideal fcc structure. When the incident angle is ±80°, ±70°, and ±60° respectively, there is a small raised peak (located around 0.67 Å) that is contributed by the reconstructed Cu atoms, as shown in Figs. 6(a)–6(c) and 6(i)–6(k). This indicates that the reconstructed Cu atoms with stress due to the nanoindenter crowd together, so that the distance between the neighbor reconstructed Cu atoms is shorter than the nearest neighbor atomic distance for the ideal Cu crystal. When the incident angle is 80° (Fig. 6(k)) the height of

the small raised peak (located at 0.68 Å) reaches the highest value (24.01) among all the small raised peaks in the Cu RDF curves. When the incident angle is −60° (Fig. 6(c)), the height of the small raised peak (located at 0.68 Å) reaches the lowest value (2.09). Due to the dynamical mechanism that is similar to that mentioned in the previous section for Si RDF, the number of reconstructed Cu atoms for 80° is larger than the other cases. However, when the incident angle is between −45° and 45°, there is no small raised peak around 0.66 Å in the Cu RDF curves. This fact happens because the vertical component of the Cu atom stress introduced by the nanoindenter with the incident angle between −45° and 45° is larger than that with ±80°, ±70°, and ±60° incident angle. The dislocation of these crowded Cu atoms for the cases with the incident angle between −45° and 45° can then get enough energy to overcome the potential barrier of diffusion, and diffuses into the deep part of the Cu bulk so that it partly releases the stress of the crowded Cu atoms and enlarges the distance between the crowded neighbor Cu atoms. The small raised peak around 0.66 Å for ±80°, ±70° and ±60° then disappears for the cases when the incident angle is between −45° and 45°. The structure with partly released stress is obviously more stable than the other cases.

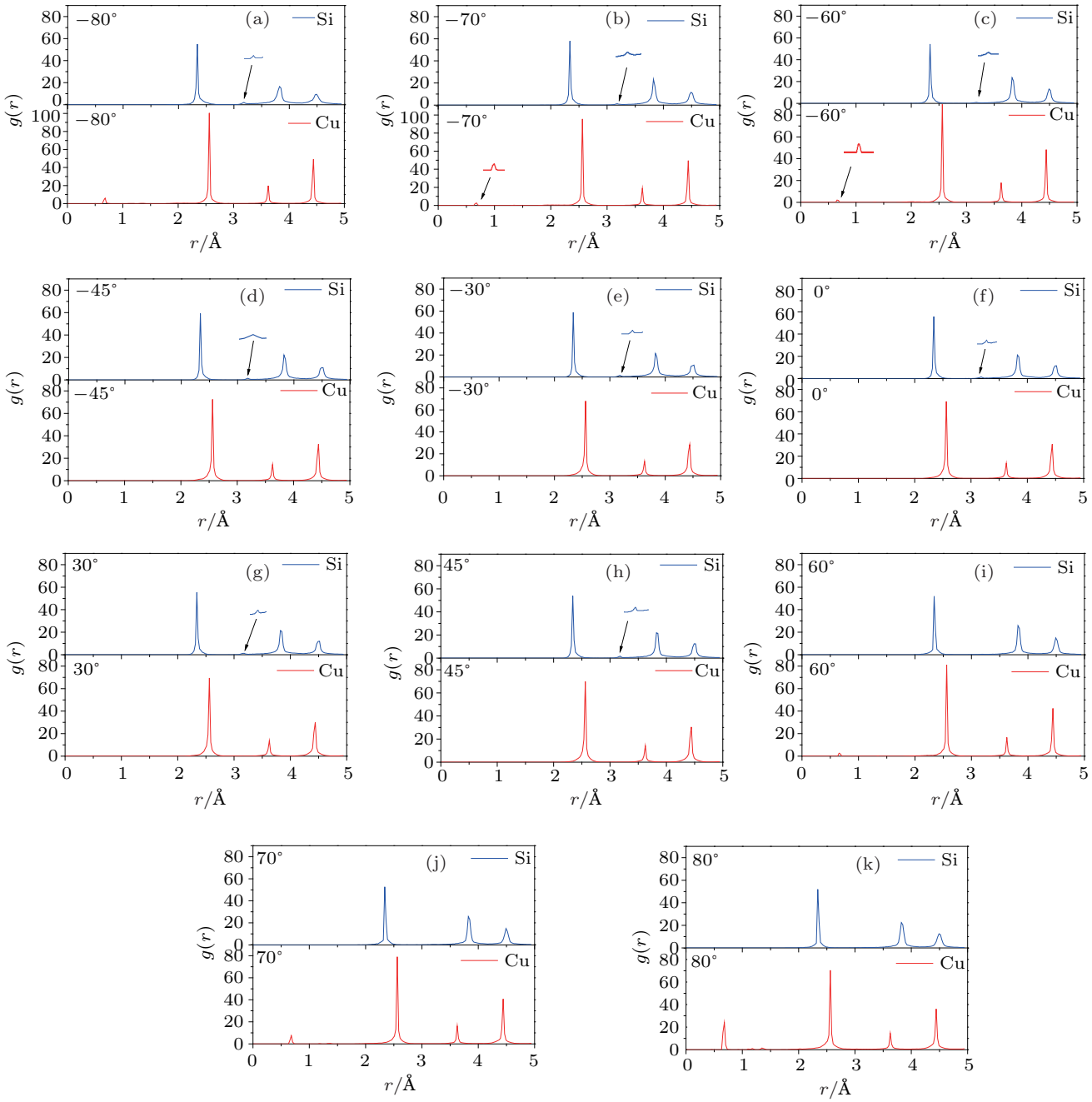


Fig. 6. (color online) The radial distribution functions for the nanoindentation depth 20 Å with different incident angles ((a)–(k)).

4. Conclusion

The structural properties of the Si/Cu heterogenous interface under nanoindenter are obtained by performing MD simulations. The results indicate that the indentation depth, the incident angle, and the size of the nanoindenter play important roles in the structural deformation of the heterogenous interface. For a certain incident angle, the nanoindenter with increasing indentation depth could firstly increase the stress of each atom at the interface and then introduce more serious structural deformation of the heterogenous interface of Si/Cu. For the 20 Å indentation depth, the nanoindenter with the increasing incident angle can induce the increase of the length of the Si or Cu extended layer. Furthermore, when the absolute value of the incident angle is larger than 60°, the length of the Si or Cu extended layer is also related to the size of the nanoindenter. In particular, when the incident angle of the nanoindenter is 80°, the length of the Cu extended atom layer is very close to the length of the nanoindenter diameter. The length of the extended atom layer will affect the IC circuit performance. In the polishing process, the most appropriate diameter of each abrasive particle should be smaller than the distance of neighbor copper wires on the IC board to avoid the overlapping of the neighbor copper wires. For the cases under the nanoindenter with the incident angle from 45° to −45°, the dislocations of the atoms under the nanoindenter can get enough energy to overcome the diffusion potential barrier, and diffuse into the deeper region of the material and cause a larger region of dislocation. The stress of these atoms is then partly released and the system of the Si/Cu heterogenous interface reaches a new balance state. This systematic study on the Si/Cu heterogenous interface may give a direction to the planarizing process of the VLSI manufacture.

Acknowledgment

Part of the calculations were performed in the High Performance Computing Center (HPCC) of Jilin University.

References

[1] Vaz C, Steinmuller S, Moutafis C, Bland J and Babkevich A Y 2007 *Surface Science* **601** 1377
[2] Hwang S F, Li Y H and Hong Z H 2012 *Comput. Mater. Sci.* **56** 85
[3] Pietsch G, Higashi G and Chabal Y 1994 *Appl. Phys. Lett.* **64** 3115
[4] Runnels S R and Eyman L M 1994 *J. Electrochem. Soc.* **141** 1698
[5] Ye Y, Biswas R, Bastawros A and Chandra A 2002 *Appl. Phys. Lett.* **81** 1875
[6] Ye Y, Biswas R, Morris J, Bastawros A and Chandra A 2003 *Nanotechnology* **14** 390
[7] Han X 2007 *Appl. Surf. Sci.* **253** 6211
[8] Han X, Hu Y and Yu S 2009 *Appl. Phys. A* **95** 899
[9] Si L, Guo D, Luo J and Lu X 2010 *J. Appl. Phys.* **107** 064310
[10] Si L, Guo D, Luo J, Lu X and Xie G 2011 *J. Appl. Phys.* **109** 084335
[11] Plimpton S 1995 *Journal of Computational Physics* **117** 1
[12] Tersoff J 1988 *Phys. Rev. B* **37** 6991
[13] Tersoff J 1989 *Phys. Rev. B* **39** 5566
[14] Nord J, Albe K, Erhart P and Nordlund K 2003 *J. Phys.: Condens. Matter* **15** 5649
[15] Foiles S, Baskes M and Daw M 1986 *Phys. Rev. B* **33** 7983
[16] Ackland G, Mendelev M, Srolovitz D, Han S and Barashev A 2004 *J. Phys.: Condens. Matter* **16** S2629
[17] Ackland G and Fox H 2005 *J. Phys.: Condens. Matter* **17** 1851
[18] Daw M S and Baskes M 1983 *Phys. Rev. Lett.* **50** 1285
[19] Daw M S and Baskes M I 1984 *Phys. Rev. B* **29** 6443
[20] Finnis M and Sinclair J 1984 *Philosophical Magazine A* **50** 45
[21] Stukowski A, Sadigh B, Erhart P and Caro A 2009 *Modelling and Simulation in Materials Science and Engineering* **17** 075005
[22] Girifalco L A and Weizer V G 1959 *Phys. Rev.* **114** 687
[23] Parrinello M and Rahman A 1981 *J. Appl. Phys.* **52** 7182
[24] Shinoda W, Shiga M and Mikami M 2004 *Phys. Rev. B* **69** 134103
[25] Martyna G J, Tobias D J and Klein M L 1994 *The Journal of Chemical Physics* **101** 4177
[26] Tuckerman M E, Alejandre J, López-Rendón R, Jochim A L and Martyna G J 2006 *J. Phys. A: Math. Gen.* **39** 5629
[27] Nosé S 1984 *The Journal of Chemical Physics* **81** 511
[28] Hoover W G 1985 *Phys. Rev. A* **31** 1695
[29] Bodapati A, Treacy M M J, Falk M, Kieffer J and Keblinski P 2006 *J. Non-Cryst. Solids* **352** 116